Supporting Information

Wang et al. 10.1073/pnas.1311249111

SI Materials and Methods

Cell Culture and Transfection. Michigan Cancer Foundation (MCF)-7, HeLa-S3, HEK293T, human MDA-MB-231 breast adenocarcinoma, and human MDA-MB-435 breast carcinoma cells were cultured in DMEM with 10% (vol/vol) heat-inactivated FBS and 1 mM sodium pyruvate and 1% nonessential amino acid at 37 °C in a 5% (vol/vol) CO_2/95% (vol/vol) air incubator. Hypoxia-cultured cells (1% O_2) were incubated in a modular incubator chamber flushed with 1% O_2 /5% (vol/vol) CO_2/balance N_2 and incubated at 37 °C. Transfection of cells was performed by using Lipofectamine 2000 (Invitrogen) according to the manufacturer's protocol. Cells were harvested 24 h posttransfection and washed in PBS for further analysis.

Establishments of Jumonji Domain-Containing Dioxygenase (JMJD)5-Expressing and JMJD5-Knockdown Cell Lines. For establishment of a stable JMJD5-expressing HeLaS3 cell line, pcDNA3-JMJD5 transfected cells were selected in G418 (800 μg/mL)-containing medium for 2 wk. The G418-resistant colonies were chosen, amplified, and evaluated the expression of Flag-JMJD5 by Western blotting with monoclonal antibody against Flag. For establishment of JMJD5-knockdown MCF-7 cell lines, the lentivirus-infected [shLKO (an empty lentiviral vector) or sh*JMJD5* constructs] MCF-7 cells were selected in puromycin (3 μg/mL)-containing media for 2 wk. The expression levels of JMJD5 of the puromycin-resistant MCF-7 cells were further evaluated by Western blotting. To down-regulate the endogenous pyruvate kinase muscle isozyme (PKM)2 expression, transfection of the siRNA-PKM2 (Santa Cruz) into MCF-7 cells was performed by using Lipofectamine RNAi-MAX (Invitrogen) according to the manufacturer's protocol. Cells were harvested 48 h posttransfection, and the expression levels of PKM2 were evaluated by Western blotting.

Plasmids. PCR-amplified human JMJD5 was cloned into pcDNA3.1-Flag as described previously (1). Full-length construct of pcDNA-HA-PKM2 was a gift from Dr. Zhimin Lu (The University of Texas, MD Anderson Cancer Center). (2). The hypoxia-inducible factor (HIF)-1α reporter that contains hypoxia-response elements (HREs) fused with a firefly luciferase (pHRE-FLuc) (3) was purchased from Addgene. Lentiviral vectors pLKO-Control and pLKO-sh*JMJD5* were used as described previously (1). The N- and C-terminal–truncated constructs of PKM2 and JMJD5 were generated from the full-length counterparts by PCR with specific primers (listed in Tables S1 and S2) and inserted into pcDNA3.1-HA and pcDNA3.1-Flag, respectively, yielding HA-PKM2 and Flag-JMJD5 truncation mutants.

Antibodies. Rabbit anti-PKM2, anti-GAPHD, anti-PCNA, and anti–HIF-1α antibodies were purchased from Cell Signaling Technology. Mouse monoclonal antibody anti–HIF-1α [chromatin immunoprecipitation (ChIP)-grade] assay was purchased from Abcam. Mouse monoclonal antibody anti-PKM2 and mouse IgG were purchased from GeneTex. Mouse monoclonal antibodies recognizing Flag, His, HA, GST, and β-actin were purchased from Sigma. The homemade rabbit anti-JMJD5 antibody was raised against a full length of recombinant PKM2. Rabbit preimmune serum was collected before immunization.

Lentivirus Production. HEK293T cells were seeded onto 10-cm culture dishes 1 d before transfection and replaced with DMEM supplemented with 1% FBS antibiotics-free medium for 30 min before transfection. Recombinant lentivirus was generated by transfection with lentiviral transducing vector encoding shLKO or sh*JMJD5* and packaging vectors pMD.G (2.5 mg) and pCMVR8.91 (7.5 mg) in HEK293T cells. After 48 h, virus particles in the medium were harvested, filtered through a 0.45-mm syringe-driven filter (Millipore), and transduced into MCF-7 cells.

Liquid Chromatography–Tandem MS and Data Process. Gel slices of proteins were further treated by in-gel digestion (4). Briefly, samples were reduced and alkylated by DTT/iodoacetamide. Each sample was digested with trypsin (wt/wt, 1:100; Promega) at 37 °C overnight. The digested peptides were injected into a MicrOTOF-Q (Bruker Daltonics) coupled to an Ultimate LC system (Thermo Fisher). Peak lists and Mascot generic format files were created using the DataAnalysis software 3.4 (Bruker Daltonics) and searched by Mascot search engine (v.2.2.03 Matrix Science) against Swiss-Prot database as previously described (5). The parameters were set as follows. The mass tolerance of the precursor and fragment ions were both 0.1 Da. Trypsin was set as the enzyme, and a maximum of three missed cleavages was allowed. Carbamidomethylation of cysteine was assumed as a fixed modification; acetylation at protein N-terminal, oxidation of methionine, and Gln change to pyro-Glu were assumed as variable modifications. After Mascot search, the resulting data were imported to the software Scaffold 3.0.7 (Proteome Software) to evaluate the information of peptide identifications and modifications. Protein identification is accepted if protein probability is >95% containing at least two peptides with peptide prophet algorithm probability of >95%.

Immunoprecipitation, GST Pull-Down, and Western Blotting Assays. Cell lysates used for immunoprecipitation (IP) assay were extracted in IP-lysis buffer [50 mM Tris·Cl (pH 7.4), 150 mM NaCl, 0.5% Nonidet P-40, 5% glycerol, 1 mM EDTA, and 1× protease inhibitors (Thermo)] at 4 °C. Supernatants were clarified by centrifugation at top speed (16,000 × *g*) for 30 min at 4 °C. The supernatants (500 μL) were incubated with the corresponding antibodies (10 μg) as indicated and 50 μL of protein A/G Dynabeads (Invitrogen) at 4 °C overnight. The beads were washed three times with IP-lysis buffer. Elution was performed by incubating the washed beads in 30 μL of 7.5 mM Tris·HCl buffer (pH 8.0), 50 mM DTT, and 1× SDS sample buffer (Bio-Rad) at 90 °C for 10 min. The input lysates and immunoprecipitates were separated by 5–15% SDS/PAGE and analyzed by light chromatography–tandem MS or Western blotting assay as described previously (6). Purified GST-JMJD5 fusion protein (20 μg) or GST control (20 μg) were mixed His-PKM2 fusion protein (20 μg) with 20 μL of preequilibrated GST-agarose (GE Healthcare) in IP-lysis buffer. The mixtures were incubated overnight at 4 °C with agitation and then washed three times with 400 μL of IP-lysis buffer before elution with 50 μL of 50 mM reduced glutathione (in 50 mM Tris·HCl, pH 8.0). Protein samples from total cell extracts, IP, GST pull down, and chemical cross-linking were separated by 10% SDS/PAGE, followed by Western blotting assay with corresponding antibodies as indicated.

Confocal Microscopic Analysis. MCF-7 and HeLaS3 cells grew on coverslips were fixed with 3.7% paraformaldehyde for 30 min and penetrated by treatment with blocking buffer (1× PBS plus 4% normal donkey serum) containing 0.1% of Triton X-100 for 1 h. PKM2 and Flag-JMJD5 (for HeLa cells) were marked with rabbit anti-PKM2 (1:1,000) and mouse anti-Flag-tag (1:2,000),

respectively. Cell nuclei were stained with DAPI. Alexa-488–conjugated anti-rabbit (1:1,000) and Cy5-conjugated anti-mouse (1:1,000) IgGs were used as secondary antibodies. Cells were examined in a Zeiss LSM 780 laser-scanning microscope (1-μm thickness) with a Plan-Apochromat 63×/1.4 oil immersion objective. Images were analyzed using the line profile tool in the LSM 780 META ZEN 2011 software package (Carl Zeiss).

Cell-Proliferation Assay. Cells were seeded in six-well plates at a density of 3×10^5 cells per well and incubated overnight. Cells were then shifted to either normoxic (20% O_2) or hypoxic (1% O_2) condition, and cell number was counted each day after the treatments. Data represent the means ± SD of three independent experiments.

Purification of GST-JMJD5 and 6XHis-PKM2. GST, GST-JMJD5, or His-PKM2 protein expression was induced with 0.2 mM isopropyl β-D-1-thiogalactopyranoside from in *Escherichia coli* BL21 (Rosetta) harboring pGEX-4T1, pGEX4T1-JMJD5, or pET-28a-PKM2 in LB-ampicillin (100 μg/mL) media at an OD of ∼0.8. Proteins were expressed for at 16 °C for 16 h. Affinity purification of the recombinant proteins were carried out at 4 °C according to previously described procedures (7). The purified proteins were resuspended in Tris buffer (50 mM Tris·HCl, pH 7.4, 150 mM, 1 mM β-mercaptoethanol, 1 mM PMSF). Protein concentrations were measured using the Bradford method (Bio-Rad).

Subcellular Fractionation. Fractionation of nuclear and cytosolic extracts was performed by using NE-PER Nuclear and Cytoplasmic Extraction kit (Thermo Scientific) according to the manufacturer's instructions.

Luciferase Activity Assay. Cells were seeded onto 48-well plates, transfected with pHRE-Firefly luciferase reporter (3), internal control reporter pTK (Thymidine kinase)-Renilla luciferase (Promega), pcDNA3.1-HA, pcDNA3.1-HA-PKM2, pcDNA3.1-HA-PKM2 (R399E), pcDNA3.1-Flag-JMJD5, or siRNA vector targeting PKM2 and exposed to 20% or 1% O2 for 24 h. Firefly and Renilla luciferase activities were determined using the Dual-Luciferase Assay System (Promega).

ChIP Assay. ChIP assays were performed by using ChIP Assay Kit (Magna ChIPG assay kit; Millipore). Briefly, 8×10^6 MCF-7 (LKO) or MCF-7 sh*JMJD5* cells were cross-linked with 1% formaldehyde for 20 min and then quenched in 0.125 M glycine for 30 min. The cell lysates were sonicated and subjected to IP using antibodies against JMJD5 (homemade rabbit polyclonal antibody), PKM2 (GeneTex, mouse monoclonal antibody), and HIF-1α (mouse monoclonal antibody; Abcam). The precipitated DNAs were analyzed and quantified by using SYBR Green Real-time PCR analysis (Applied Biosystems StepOne). Primer sequences are listed in Tables S1 and S2. Fold enrichment was calculated based on threshold cycle (Ct) as $2^{-\Delta(\Delta Ct)}$, where ΔCt = Ct (IP) − Ct (input) and Δ(ΔCt) = ΔCt (antibody) − ΔCt (IgG).

Re-ChIP. MCF-7 cells cultured in DMEM supplemented with 10% FCS were cotransfected with human Flag-JMJD5 and HA-PKM2 followed by exposure to hypoxia for 24 h. Chromatin obtained from $\sim 8 \times 10^7$ MCF-7 cells was cross-linked with 1% formaldehyde for 30 min and then quenched in 0.125 M glycine for 30 min. Re-ChIP was conducted according to the manufactory's protocols with mild modification. ChIP assays were conducted according to the manufacturer's instruction (Magna ChIPG assay kit, Millipore) with antibody against Flag (Sigma) or HA (Santa Cruz Biotechnology) as indicated. The precipitated DNAs were analyzed and quantified by using SYBR Green Real-time PCR analysis (Applied Biosystems StepOne). Primer sequences are listed in Tables S1 and S2. Fold enrichment was calculated based on Ct as $2^{-\Delta(\Delta Ct)}$, where ΔCt = Ct (IP) − Ct (Input) and Δ(ΔCt) = ΔCt (Antibody) − ΔCt (IgG). PCR products designed to amplify regions specific to the human *LDHA* promoters were analyzed on 1.8% (wt/vol) agarose/Tris-acetate-EDTA gels with ethidium-bromide stain.

Quantitative Real-Time PCR. Total RNAs were extracted with TRIzol (Invitrogen) reagent, and the cDNAs were prepared using the SuperScript First-strand cDNA Synthesis Kit (Invitrogen). Real-time quantitative (qRT)-PCR analysis was performed with ABI SYBR Green Master (ABI) using the 7500 Fast Real-Time PCR System (Applied Biosystems). Data were normalized to the expression of *GAPDH*. Quantitative PCR primers are listed in Tables S1 and S2.

Surface Plasmon Resonance Assay. Purified His-PKM2 and Flag-JMJD5 proteins were resuspended in sodium phosphate buffer (pH 7.3). The automated Biacore-T100 (GE Healthcare) instrument was used for measuring JMJD5-PKM2 interaction. For immobilizing GST-JMJD5 on a sensor chip by amine coupling, according to the software wizards for Biacore T100, the carboxylated dextran CM5 sensor chip was activated by treatment with 1:1 (vol/vol) mixture of 50 mM NHS and 200 mM ethyl(dimethylaminopropyl) carbodiimide, followed by passing through a 50 μg/mL of GST-JMJD5 protein in 50 mM sodium acetate buffer (pH 5.0). The immobilization process was then blocked by injection of 1 M ethanolamine·HCl (pH 8.5) at a flow rate of 5 μL/min. The binding and kinetic assays were carried out in 100 mM sodium phosphate buffer (pH 7.3) containing 100 mM NaCl at a flow rate of 30 μL/min, and contact time was 250 s. The concentrations of PKM2 (analyte) were used ranging from 0.195 to 100 μM. Dissociation was initiated by replacing the analyte with buffer. The association and dissociation curves were monitored for 550 s. Immobilized JMJD5 protein was regenerated with an injection of 100 mM sodium phosphate (pH 7.3) containing 1 M NaCl for 30 s. All experiments were conducted at 25 °C. Sensograms were obtained and analyzed with Biacore T100 evaluation software.

In Vitro PKM2 Activity Assay. Purified His_6-PKM2 (10 μM) and GST-JMJD5 (10 μM) proteins were resuspended in sodium phosphate buffer (pH 7.3). For monitoring the inhibitory effect of GST-JMJD5 on His-PKM2 activity, PKM2 (10 nM) was coincubated with various concentrations of GST-JMJD5 (0–1,500 nM). The PKM2 activities were measured with a colorimetric-based pyruvate kinase activity assay kit (BioVision) according to the manufacturer's protocol.

Glucose Uptake Assay. MCF-7 cells transduced with lentivirus encoding shLKO or sh*JMJD5* (LKO and sh*JMJD5* cell lines, respectively) were cultured in glucose-free DMEM for 24 h and then incubated with high-glucose DMEM for 1 h. The intracellular glucose was measured with a fluorescence-based glucose assay kit (BioVision,) according to the manufacturer's protocol.

Lactate Production Assay. MCF-7 cells transduced with lentivirus encoding shLKO or sh*JMJD5* (LKO and sh*JMJD5* cell lines, respectively) were incubated with FBS-free DMEM for 1 h. The extracellular lactate was measured in the medium with a fluorescence-based lactate assay kit (BioVision) according to the manufacturer's protocol.

Statistical Analysis. Data were expressed as means ± SD. The significance of difference was examined by Student *t* test (two-tailed). $P < 0.05$ was considered to be significant.

Chemical Cross-Linking Assay. HEK293T cells that cotransfected HA-PKM2 plus Flag-JMJD5, HA-PKM2 plus Flag-JMJD5ΔN80, HA-PKM2 alone, or Flag-JMJD5 alone were lysed with sodium

phosphate buffer (pH 7.3) containing 0.5% Triton X-100 and 1× protease inhibitors (Thermo) for 30 min at 4 °C. Crude cell lysates were clarified by centrifugation at top speed (16, 000 × *g*) for 30 min at 4 °C. For carrying out cross-linking reactions, the supernatants (4 mg/mL) were treated with 0.01% or glutaraldehyde for various time periods (0–5 min) at 37 °C or 25 °C. The reactions were terminated by adding 1 M Tris buffer to a final concentration of 50 mM Tris·Cl (pH 8.0). Samples were then separated by 5–15% SDS/PAGE and analyzed by Western blotting with anti-HA or anti-Flag antibodies as indicated.

1. Hsia DA, et al. (2010) KDM8, a H3K36me2 histone demethylase that acts in the cyclin A1 coding region to regulate cancer cell proliferation. *Proc Natl Acad Sci USA* 107(21): 9671–9676.
2. Luo W, et al. (2011) Pyruvate kinase M2 is a PHD3-stimulated coactivator for hypoxia-inducible factor 1. *Cell* 145(5):732–744.
3. Emerling BM, Weinberg F, Liu JL, Mak TW, Chandel NS (2008) PTEN regulates p300-dependent hypoxia-inducible factor 1 transcriptional activity through Forkhead transcription factor 3a (FOXO3a). *Proc Natl Acad Sci USA* 105(7):2622–2627.
4. Tsai MH, et al. (2012) Identification of secretory gelsolin as a plasma biomarker associated with distant organ metastasis of colorectal cancer. *J Mol Med (Berl)* 90(2): 187–200.
5. Chi LM, et al. (2009) Enhanced interferon signaling pathway in oral cancer revealed by quantitative proteome analysis of microdissected specimens using $^{16}O/^{18}O$ labeling and integrated two-dimensional LC-ESI-MALDI tandem MS. *Mol Cell Proteomics* 8(7): 1453–1474.
6. Wang HJ, Cheng WC, Cheng HH, Lai CH, Wang WC (2012) Helicobacter pylori cholesteryl glucosides interfere with host membrane phase and affect type IV secretion system function during infection in AGS cells. *Mol Microbiol* 83(1):67–84.
7. Cheng WC, et al. (2012) Structures of Helicobacter pylori shikimate kinase reveal a selective inhibitor-induced-fit mechanism. *PLoS ONE* 7(3):e33481.

Fig. S1. Analysis of cellular metabolites in the glucose metabolism for MCF7 control and MCF-7–*JMJD5*–knockdown cells. MCF-7–LKO (white bar), MCF-7–sh*JMJD5*#1 (black bar), and MCF-7–sh*JMJD5*#3 (oblique bar) were cultured for 24 h under normoxia or hypoxia. Lysates were then prepared for the measurement of the following metabolites: glucose-6-phosphate (G6P); fructose 1,6 bisphosphate (F1,6BP); glucose-1-phosphate (G1P); and ribose-5-phosphate (R5P). The fold changes were measured and expressed as a ratio of LKO normoxia levels. Statistical analysis was assessed by Student *t* test. $*P < 0.05$; $**P < 0.01$.

Fig. S2. HeLa-Flag-JMJD5–expressing cells exhibited a lower level of H3K36me2 methyl mark. (*A*) JMJD5-expressing HeLa-S3 cells. Cells were fixed and stained with anti-Flag (Flag-JMJD5), anti-H3K36me2 (H3K36me2), and 4′,6-diamidino-2-phenylindole (DAPI), respectively. Purple in the merged images (merge) indicates colocalization of H3K36me2 and DAPI. The corresponding differential interference contrast microscopy (DIC) images are shown in the right. Clones 2D and 3B: selected stable cell clones expressing Flag-JMJD5. Mixture: cells transfected with pCDNA-Flag-JMJD5 without performing single-clone selection and amplification; mock: cells transfected with pcDNA-flag. (Scale bars, 10 μm.) (*B*) Western blotting analysis of whole-cell lysates from mock cells (Mock-EV) and selected lines (HeLa-2D, -3B, -5C, and -3D) using mouse anti-Flag antibody. HeLa-S3, cells without transfection.

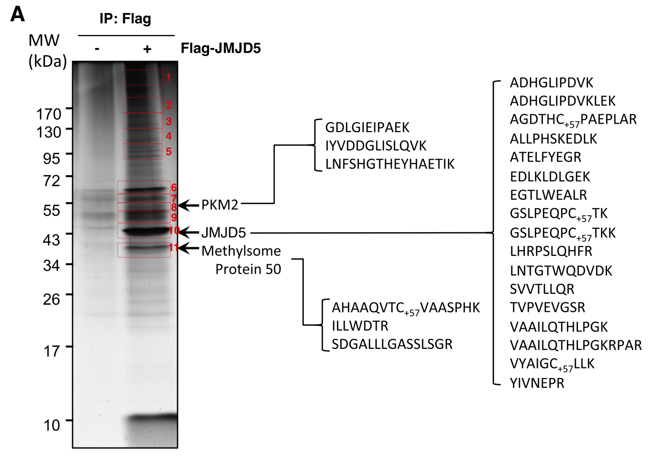

B

Supplemental Information: Fig. S3B. Proteins and peptides identified from Fig. 2A (left figure) by in-gel-digestion.

We cut 11 band slices from the lane of Flag-JMJD5 and also in the lane of Flag control. As the results showed, we identified 20 proteins from 4 bands which were differentially expressed in the lane of flag-JMJD5 transfection when comparing to control.

Band	Protein name	Protein ID details		Peptide start index	Peptide stop index	Peptide sequence	Mascot Ion score	Mascot Identity score	Modifications identified by spectrum	Actual peptide mass (AMU)	Spectrum charge	Actual minus calculated peptide mass	Actual minus calculated peptide mass
1	DNA-dependent protein kinase catalytic subunit	Molecular weight	469077.5	914	924	VTELALTASDR	42.2	32.2		1,174.62	2	0.0036	3.1
		Protein identification probability	100.00%	2107	2120	SLGPPQGEEDSVPR	41.6	30.7		1,466.69	2	-0.0059	-4
		Peptide identification probability	95.00%	3325	3335	DQNILLGTTYR	48	31.9		1,292.65	2	-0.023	-17
		Sequence coverage (%)	1% (36/4128)										
		Number of unique peptides	3										
		Number of unique spectra	3										
		Number of total spectra	4										
	RE1-silencing transcription factor	Molecular weight	121852	200	213	ESGSSTAEEGDFSK	24.9	25.3		1,429.59	2	0.0097	6.8
		Protein identification probability	100.00%	228	236	YDHYTAHLK	34.6	31.5		1,146.55	2	0.0012	1
		Peptide identification probability	95.00%	334	349	CDQCSYVASNQHEVTR	52.5	25	Carbamidomethyl (+57), Carbamidomethyl (+57)	1,952.81	2	-0.0029	-1.5
		Sequence coverage (%)	10% (108/1097)	379	387	HVELHVNPR	40.6	31.9		1,099.58	2	-0.0054	-4.9
		Number of unique peptides	9	388	400	QFNCPVCDYAASK	38.8	25.3	Carbamidomethyl (+57), Carbamidomethyl (+57)	1,558.64	2	-0.0096	-6.1
		Number of unique spectra	9	402	409	CNLQYHFK	36.2	30.8	Carbamidomethyl (+57)	1,108.52	2	0.011	10
		Number of total spectra	13	434	445	EADLPDNITNEK	52.8	30.5		1,357.63	2	-0.0041	-3
				478	491	KPSNNVSVIQVTTR	47.2	30		1,541.84	2	-0.012	-7.8
				834	846	EQVLIEVGLVPVK	47	25.2		1,421.84	2	-0.0082	-5.8
	Telomere-associated protein RIF1	Molecular weight	274451.3	520	532	EKPGSEVLTLLLK	33.2	26.6		1,425.83	2	-0.011	-7.8
		Protein identification probability	100.00%	1489	1504	TLGETSANAETEQNKK	32.4	31.2		1,719.86	2	0.028	16
		Peptide identification probability	95.00%	1576	1588	SNESVDIQDQEEK	35.2	27.2		1,519.65	2	-0.018	-12
		Sequence coverage (%)	2% (54/2472)	2189	2200	SQEDEISSPVNK	29.3	30.8		1,331.62	2	0.0034	2.6
		Number of unique peptides	4										
		Number of unique spectra	4										
		Number of total spectra	6										
8	Heterogeneous nuclear ribonucleoprotein K	Molecular weight	50960.5	70	86	TDYNASVSVPDSSGPER	42.7	29.5		1,779.81	2	0.016	9
		Protein identification probability	100.00%	192	201	VVLIGGKPDR	32.1	27		1,052.63	2	-0.0078	-7.4
		Peptide identification probability	95.00%	208	219	IILDLISESPIK	57.4	28.1		1,339.78	2	-0.021	-15
		Sequence coverage (%)	8% (39/463)										
		Number of unique peptides	3										
		Number of unique spectra	3										
		Number of total spectra	3										
	Non-POU domain-containing octamer-binding protein	Molecular weight	54213.6	100	107	AGEVFIHK	40.2	31.2		899.48	2	-0.0021	-2.4
		Protein identification probability	100.00%	191	202	GIVEFSGKPAAR	29.9	32		1,230.65	2	-0.017	-14
		Peptide identification probability	95.00%	326	336	MEELHNQEVQK	26	30.1		1,383.63	2	-0.011	-8.1
		Sequence coverage (%)	9% (43/471)	457	468	AAPGAEFAPNKR	29.3	31.8		1,227.63	2	-0.0083	-6.8
		Number of unique peptides	4										
		Number of unique spectra	4										
		Number of total spectra	6										
	Pyruvate kinase isozymes M1/M2	Molecular weight	57919.5	74	89	LNFSHGTHEYHAETIK	25.2	30.2		1,882.90	2	0.00082	0.43
		Protein identification probability	100.00%	174	186	IYVDDGLISLQVK	46.5	30.4		1,461.80	2	-0.012	-8.5
		Peptide identification probability	95.00%	295	305	GDLGIEIPAEK	42.3	31.1		1,140.60	2	-0.0014	-1.2
		Sequence coverage (%)	8% (40/531)										
		Number of unique peptides	3										
		Number of unique spectra	3										
		Number of total spectra	3										
	U4/U6 small nuclear ribonucleoprotein Prp31	Molecular weight	55439.4	77	91	ASEVMGPVEAAPEYR	77.7	30		1,604.74	2	-0.014	-8.6
		Protein identification probability	100.00%	204	211	IYEYVESR	28.9	30.5		1,057.50	2	-0.0088	-8.3
		Peptide identification probability	95.00%	231	243	IMGVAGGLTNLSK	38.8	31.1		1,259.69	2	-0.0041	-3.3
		Sequence coverage (%)	12% (60/499)	316	326	VGYELKDEIER	64.4	32.3		1,349.68	2	-0.0048	-3.5
		Number of unique peptides	5	339	351	QVKPLPAPLDGQR	37.3	30.1	Gln->pyro-Glu (-17)	1,400.78	2	-0.0027	-2
		Number of unique spectra	5										
		Number of total spectra	12										
10	60S ribosomal protein L3	Molecular weight	46091.5	104	115	TVFAEHISDECK	26.2	29.1	Carbamidomethyl (+57)	1,434.64	2	-0.0065	-4.5
		Protein identification probability	99.80%	301	312	NNASTDYDLSDK	34.1	26.4		1,341.56	2	-0.0068	-5.1
		Peptide identification probability	95.00%										
		Sequence coverage (%)	6% (24/403)										
		Number of unique peptides	2										
		Number of unique spectra	2										
		Number of total spectra	2										
	Elongation factor 1-alpha 1	Molecular weight	50123.2	21	30	STTTGHLIYK	41.2	31.9		1,119.60	2	0.0082	7.4
		Protein identification probability	100.00%	85	96	YYVTIIDAPGHR	64	31.5		1,403.72	2	-0.0048	-3.4
		Peptide identification probability	95.00%	135	146	EHALLAYTLGVK	52.5	30.4		1,313.73	2	-0.0058	-4.4
		Sequence coverage (%)	12% (54/462)	256	266	IGGIGTVPVGR	33.7	28.7		1,024.59	2	-0.013	-12
		Number of unique peptides	5	431	439	QTVAVGVIK	52.3	29.2		913.56	2	-0.0033	-3.6
		Number of unique spectra	5										
		Number of total spectra	8										
	Elongation factor 1-gamma	Molecular weight	50101.4	18	30	ALIAAQYSGAQVR	28.7	31.2		1,346.73	2	-0.0023	-1.7
		Protein identification probability	100.00%	286	295	STFVLDEFKR	51.7	31.1		1,240.64	2	-0.0017	-1.4
		Peptide identification probability	95.00%										
		Sequence coverage (%)	5% (23/437)										
		Number of unique peptides	2										
		Number of unique spectra	2										
		Number of total spectra	2										
	Eukaryotic initiation factor 4A-III	Molecular weight	46854.4	2	14	ATTATMATSGSAR	29.9	30.5	Acetyl (+42)	1,266.58	2	-0.0038	-3
		Protein identification probability	100.00%	106	116	ETQALILAPTR	54	30.1		1,211.67	2	-0.015	-12
		Peptide identification probability	95.00%	152	166	KLDYGQHVVAGTPGR	32.2	30.9		1,596.82	2	-0.015	-9.4
		Sequence coverage (%)	9% (39/411)	153	166	LDYGQHVVAGTPGR	29.3	31		1,468.73	2	-0.014	-9.6
		Number of unique peptides	4										
		Number of unique spectra	4										
		Number of total spectra	5										
	JmjC domain-containing protein 5	Molecular weight	47252.9	2	14	AGDTHCPAEPLAR	30.7	30.5	Carbamidomethyl (+57)	1,393.64	2	0.0015	1.1
		Protein identification probability	100.00%	15	23	EGTLWEALR	72.2	32.9		1,073.55	2	-0.002	-1.9
		Peptide identification probability	95.00%	24	34	ALLPHSKEDLK	26.8	29.6		1,249.70	2	-0.0046	-3.7
		Sequence coverage (%)	34% (142/416)	31	40	EDLKLDLGEK	37.8	32.4		1,158.61	2	-0.00026	-0.23
		Number of unique peptides	17	44	51	SVVTLLQR	38.9	30.8		914.55	2	-0.0088	-9.6
		Number of unique spectra	18	52	60	ATELFYEGR	40.8	30.3		1,084.51	2	-0.011	-10
		Number of total spectra	30	79	89	LNTGTWQDVDK	34.9	31.6		1,275.62	2	0.012	9.2
				94	102	VYAIGCLLK	27.5	30.9	Carbamidomethyl (+57)	1,035.57	2	-0.0059	-5.7
				141	152	VAAILQTHLPGK	46.6	28.9		1,246.72	2	-0.023	-18
				141	156	VAAILQTHLPGKRPAR	32.4	25		1,727.02	3	-0.0083	-4.8
				157	166	GSLPEQPCTK	33.6	31.1	Carbamidomethyl (+57)	1,115.54	2	0.0092	8.2
				157	167	GSLPEQPCTKK	33.2	31.5	Carbamidomethyl (+57)	1,243.62	2	-0.0036	-2.9
				170	179	ADHGLIPDVK	56.3	32.1		1,063.57	2	-0.0014	-1.4
				170	182	ADHGLIPDVKLEK	30.4	30.5		1,433.78	3	-0.011	-8
				187	196	LHRPSLQHFR	28.2	31		1,289.71	2	-0.0042	-3.2
				234	242	TVPVEVGSR	35.6	31.6		942.51	2	-0.0071	-7.6
				262	268	YIVNEPR	39.2	33.2		889.47	2	0.0027	3.1
	Serine/threonine-protein kinase 38	Molecular weight	54174.2	51	62	VMEEEGLKDEEK	54.6	29.8		1,434.65	2	-0.0056	-3.9
		Protein identification probability	100.00%	360	367	FCCEWEHR	25.7	25	Carbamidomethyl (+57), Carbamidomethyl (+57)	1,222.44	2	-0.021	-17
		Peptide identification probability	95.00%										
		Sequence coverage (%)	4% (20/465)										
		Number of unique peptides	2										
		Number of unique spectra	2										
		Number of total spectra	2										
11	Actin, cytoplasmic 1 or 2	Molecular weight	41719.8	19	28	AGFAGDDAPR	58.6	28.9		975.43	2	-0.013	-13
		Protein identification probability	100.00%	51	61	DSYVGDEAQSK	26.3	28.1		1,197.51	2	-0.00072	-0.6
		Peptide identification probability	95.00%	197	206	GYSFTTTAER	32	29.3		1,131.51	2	-0.012	-10
		Sequence coverage (%)	11% (42/375)	316	326	EITALAPSTMK	33.9	32.3	Oxidation (+16)	1,176.60	2	-0.011	-9.3
		Number of unique peptides	4	316	326	EITALAPSTMK	39.2	32.5		1,160.59	2	-0.018	-16
		Number of unique spectra	4										
		Number of total spectra	10										
	Histone H1.2, 1.3 or 1.4	Molecular weight	21347.8	35	46	ASGPPVSELITK	49.5	30.5		1,197.66	2	-0.0054	-4.5
		Protein identification probability	99.80%	65	75	ALAAAGYDVEK	41.5	32.4		1,106.56	2	0.0025	2.3
		Peptide identification probability	95.00%										
		Sequence coverage (%)	11% (23/213)										
		Number of unique peptides	2										
		Number of unique spectra	2										
		Number of total spectra	2										
	Interleukin enhancer-binding factor 2	Molecular weight	43044	197	206	VLQSALAAIR	48.9	27.6		1,040.62	2	-0.0097	-9.3
		Protein identification probability	99.80%	260	269	QPLALNVAYR	31.1	32		1,143.62	2	-0.022	-19
		Peptide identification probability	95.00%										
		Sequence coverage (%)	5% (20/390)										
		Number of unique peptides	2										
		Number of unique spectra	2										
		Number of total spectra	2										
	Methylosome protein 50	Molecular weight	36705	165	179	AHAAQVTCVAASPHK	41.4	31.1	Carbamidomethyl (+57)	1,546.76	2	-0.008	-5.2
		Protein identification probability	100.00%	192	198	ILLWDTR	41.7	32.8		915.51	2	-0.013	-14
		Peptide identification probability	95.00%										
		Sequence coverage (%)	6% (22/342)										
		Number of unique peptides	2										
		Number of unique spectra	2										
		Number of total spectra	3										
	Poly(rC)-binding protein 1	Molecular weight	37480	47	57	INISEGNCPER	44.9	28.8	Carbamidomethyl (+57)	1,287.58	2	-0.013	-9.6
		Protein identification probability	99.80%	315	325	[illegible]	50.5	31		1,085.53	2	-0.02	-18
		Peptide identification probability	95.00%										
		Sequence coverage (%)	6% (22/356)										
		Number of unique peptides	2										
		Number of unique spectra	2										
		Number of total spectra	2										
	Protein phosphatase 1B	Molecular weight	52624	130	142	SGSTAVGVMISPK	29	32		1,232.61	2	-0.031	-25
		Protein identification probability	100.00%	143	153	HIYFINCGDSR	38.7	27.7	Carbamidomethyl (+57)	1,380.59	2	-0.033	-24
		Peptide identification probability	95.00%	180	191	IQNAGGSVMIQR	39.1	31.7		1,272.65	2	-0.015	-12
		Sequence coverage (%)	10% (47/479)	309	319	DSELDKHLESR	33	30.8		1,327.63	2	-0.006	-4.5
		Number of unique peptides	4										
		Number of unique spectra	4										
		Number of total spectra	4										
	RCC1 domain-containing protein 1	Molecular weight	40060	60	72	[illegible]	52.7	32.3		1,174.59	2	-0.0029	-2.5
		Protein identification probability	100.00%	134	141	LPLLPCAR	26	29.6	Carbamidomethyl (+57)	938.53	2	-0.012	-12
		Peptide identification probability	95.00%	187	202	HSQLGHGTLEAELEPR	31.2	30.6		1,742.85	3	-0.017	-9.6
		Sequence coverage (%)	10% (42/376)	248	258	NLAEDGETVAR	50.8	31.2		1,173.56	2	-0.0038	-3.2
		Number of unique peptides	4	259	271	EATELNEDGSQVK	54.2	29.8		1,418.64	2	-0.01	-7.1
		Number of unique spectra	[illegible]	259	272	EATELNEDGSQVKR	39.8	30.5		1,574.74	3	-0.013	-8.3
		Number of total spectra	19										

Fig. S3. Identification of PKM2 that interacts with JMJD5 by mass spectrometric analysis. (*A*) Nuclear extracts were prepared from HeLa-Mock cells (denoted as "-") or HeLa-Flag-JMJD5 (denoted as "+"), followed by IP with anti-Flag-affinity beads and eluted with Flag peptides. The elutes were resolved on SDS/PAGE. The protein bands were retrieved and analyzed by mass spectrometry. (*B*) The list of JMJD5-associated proteins.

Fig. S4. PKM2 hydroxylation is independent of JMJD5. HEK293T cells were cotransfected with the expression vectors as indicated and cultured under normoxia for 24 h, followed by IP with anti-HA and Western blotting using anti–Pro-OH (*Upper*) or anti-PKM2 (*Lower*).

Fig. S5. Subcellular localization of PKM2 in HeLa-Mock (Mock) and HeLa-Flag-*JMJD5* (HeLa-JMJD5) cells. Cells were fixed and immunostained with anti-PKM2 (green), 4′,6-diamidino-2-phenylindole that stained the nucleus (DAPI; red), and anti-Flag (JMJD5; white) that marked JMJD5, respectively. Merged images are shown as indicated (rows 4–6). The framed region of row 6 is magnified, and the images are shown in the row 7. The average mean fluorescence intensity (MFI) of PKM2 was measured by line profile tool in ZEN 2011 software (Carl Zeiss). (Scale bars, 10 μm.)

Fig. S6. Size-exclusion chromatographic analysis of the effect of JMJD5 on PKM2 oligomerization. (*A* and *B*) The peak elution positions of the individual proteins, PKM2 (tetramer), R399E (dimer only), JMJD5-FL, and JMJD5-ΔN80 (unable to bind PKM2) are shown. (*C*) The elution profiles of addition of JMJD5WT but not ΔN80 mutant into PKM2 dramatically diminishes the level of tetramer, resulting in the formation of PKM2 dimer or PKM2/JMJD5 heterodimer. (*D*) Analysis of the effect of JMJD5 on PKM2 oligomerization in vivo using MCF7 wild-type (WT)/MCF-7–sh*JMJD5* cells. There is a significant portion of tetrameric PKM2 in the cytosol of both cell types. Nuclear PKM2 is found only in wild type cells, which elutes at positions corresponding to either PKM2 dimer of PKM2/JMJD5 heterodimer. Knockdown of JMJD5 nearly completely hinders the nuclear translocation of PKM2, as evidenced by the lack of PKM2 band in the Western

Legend continued on following page

blot. Fractions of the peak (Superdex 200 26/10 column; PBS solution; flow rate, 1 mL/min) were analyzed by SDS/PAGE gels, followed by Coomassie brilliant blue staining (*A*–*C*) or immunoblotting using anti-PKM2 (*D*). Cyto, cytosolic fraction; NE, nuclear fractions.

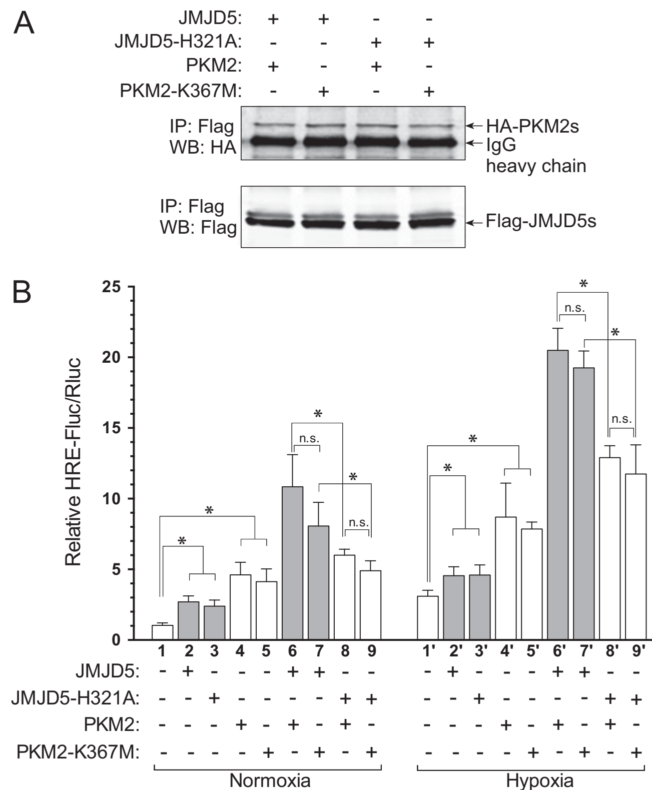

Fig. S7. Analysis of catalytically inactive JMJD5's role in HIF-1α transactivation activity. (*A*) HEK293T cells were transfected with the vectors as indicated, followed by immunoblotting analysis with anti-HA and anti-Flag, respectively. (*B*) Transactivation activity of LKO cells cotransfected with pHRE-Fluc, pTK-Rluc, and empty vector or expression vectors (JMJD5, JMJD5-H321A, PKM2, PKM2-K367M) as indicated. The ratio of Fluc:Rluc activity was normalized to LKO with the empty vector at normoxia (mean ± SD; $n = 4$). The ratio of Fluc:Rluc activity was normalized to that with the empty vector under normoxia. *$P < 0.05$.

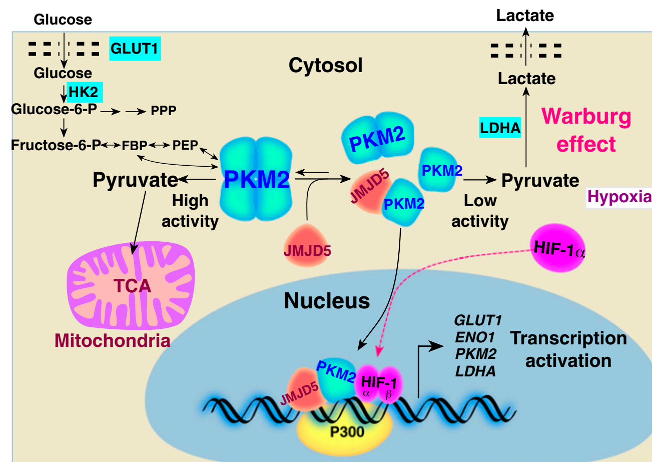

Fig. S8. The proposed model that connects JMJD5 and PKM2 in the HIF-1α system that mediates the Warburg effect.

Table S1. Primer sequences used for qRT-PCR and ChIP in this study

Primer name	Sequence (5′ to 3′)	Source
qRT-PCR		
GLUT1	Fw: CGGGCCAAGAGTGTGCTAAA	Ref. 2
	Rev: TGACGATACCGGAGCCAATG	
ENO1	Fw: TGCGTCCACTGGCATCTAC	This study
	Rev: CAGAGCAGGCGCAATAGTTTTA	
PKM2	Fw: TTGCAGCTATTCGAGGAACTCCG	Ref. 2
	Rev: CACGATAATGGCCCCACTGC	
LDHA	Fw: ATCTTGACCTACGTGGCTTGGA	
	Rev: CCATACAGGCACACTGGAATCTC	
PDK1	Fw: ACCAGGACAGCCAATACAAG	
	Rev: CCTCGGTCACTCATCTTCAC	
MCT4	Fw: TCACGGGTTTCTCCTACGC	This study
	Rev: GCCAAAGCGGTTCACACAC	
HIF-1α	Fw: CCATTAGAAAGCAGTTCCGC	This study
	Rev: TGGGTAGGAGATGGAGATGC	
18S rRNA	Fw: CGGCGACGACCCATTCGAAC	Ref. 2
	Rev: GAATCGAACCCTGATTCCCCGTC	
ChIP		
LDHA-HRE	Fw: TTGGAGGGCAGCACCTTACTTAGA	Ref. 2
	Rev: GCCTTAAGTGGAACAGCTATGCTGAC	
PKM2-HRE	Fw: TTCCTGCCTCTTGGTATGAC	
	Rev: CGGCTTGTTCCCTCCTAC	
RPL13A–non-HRE	Fw: GAGGCGAGGGTGATAGAG	
	Rev: ACACACAAGGGTCCAATTC	

Fw, forward; Rev, reverse.

Table S2. Primer sequences used for constructing truncated PKM2 and JMJD5

Primer name	Sequence (5′ to 3′)	RE	Location*	Source
PKM2-HA-F	Fw: TTTCGGTCCGATGTCGAAGCCCCATAGT	CpoI	85–102	This study
PKM2-R	Rev: TTTCTCGAGTCACGGCACAGGAACAAC	XhoI	1663–1653	
PKM2-d55-f	Fw: TTTCGGTCCGCGATCAGTGGAGACGTTG	CpoI	250–267	
PKM2-d110-f	Fw: TTTCGGTCCGGCTCTAGACACTAAAGGAC	CpoI	414–443	
PKM2-d165-f	Fw: TTTCGGTCCGAAGGTGGTGGAAGTGGGC	CpoI	580–597	
PKM2-d55-r	Rev: TTTCTCGAGTCAGTCCTTGCACAGCACAGG	XhoI	1512–1495	
PKM2-d110-r	Rev: TTTCTCGGAGGCCTCCACGGCACC	XhoI	1344–1326	
PKM2-d160-r	Rev: TTTCTCGAGTCAGGCTGTTTCTCCAGACAG	XhoI	1182–1165	
JMJD5-Flag-F	Fw: TTTGAATTCATGGCTGGAGACACCCAC	EcoRI	233–250	
JMJD5-R	Rev: TTTCTCGAGCTACGACCACCAGAAGCT	XhoI	1483–1466	
JMJD5-d40-f	Fw: TTTGAATTCGTGGAGAGGAGCGTGGTG	EcoRI	353–370	
JMJD5-d80-f	Fw: TTTGAATTCACGGGCACATGGCAGGAC	EcoRI	473–490	
JMJD5-d120-f	Fw: TTTGAATTCCGGGTCTGTGACATGGGC	EcoRI	593–610	
JMJD5-d40-r	Rev: TTTCTCGAGAAACTTGGGGAACTTTTC	XhoI	1360–1343	
JMJD5-d80-r	Rev: TTTCTCGAGCTTCCTCCCCATCACCTG	XhoI	1340–1223	
JMJD5-d120-r	Rev: TTTCTCGAGGCTGCAGTAGTCGGGGAT	XhoI	1021–1103	
PKM-K367M-f	Fw: GCTGTCTGGAGAAACAGCCATGGGGGACTATCCTCTGGAGG	BamH1	1080–1117	Ref. 1
PKM-K367M-r	Rev: CCTCCAGAGGATAGTCCCCCATGGCTGTTTCTCCAGACAGC	XhoI	1117–1080	

Fw, forward; RE, restriction enzyme; Rev, reverse.
*Based on human PKM2 and JMJD5 (GenBank accession nos. NM_002654 and NP_001145348, respectively).

1. Yang W, et al. (2011) Nuclear PKM2 regulates β-catenin transactivation upon EGFR activation. *Nature* 480(7375):118–122.